Thorax 1996;**51**(Suppl 2):S16–S22

^{18}F-Fluorodeoxyglucose PET scans in lung cancer

J M B Hughes

Department of Medicine, Hammersmith Hospital, Royal Postgraduate Medical School, London, UK

Introductory article

Mediastinal staging of non-small-cell lung cancer with positron emission tomography

R Chin Jr, R Ward, JW Keyes Jr, RH Choplin, JC Reed, S Wallenhaupt, AS Hudspeth, EF Haponik

To determine the usefulness of positron emission tomography with fluoro-2-deoxyglucose (PET-FDG) in assessing mediastinal disease in patients with non-small-cell lung cancer (NSCLC) and to compare its yield to that of computed tomography (CT), we performed a prospective consecutive sample investigation in a university hospital and its related clinics. In 30 patients with NSCLC with clinical stage I (T1–2, N0, M0) disease, we compared the results of chest CT and PET-FDG with the findings at surgical exploration of the mediastinum. Seven (77%) of nine patients with surgically proven mediastinal metastasis were identified by the PET-FDG results, with four false-positives in 21 patients with negative lymph-node dissections (P=0·004). Using the results of pathologic examination of mediastinal lymph nodes as the criterion standard, the diagnostic sensitivity, specificity, accuracy, positive predictive value (PPV), and negative predictive value (NPV) for PET-FDG imaging of mediastinal metastases were 78%, 81%, 80%, 64%, and 89%, respectively. The sensitivity, specificity, accuracy, PPV, and NPV for chest CT in the detection of mediastinal metastasis were 56%, 86%, 77%, 63%, and 87%, respectively. CT and PET-FDG results agreed in 21 patients. The diagnostic accuracy of the combined imaging modalities was 90%. We concluded that mediastinal uptake of FDG correlates with the extent of mediastinal involvement of NSCLC and may contribute to preoperative staging. PET-FDG imaging complements chest CT in the noninvasive evaluation of NSCLC, and strategies for its use merit further investigation. (*Am J Respir Crit Care Med* 1995;**152**:2090–6)

The diagnosis and staging of lung cancer are everyday problems for chest physicians. The introductory article by Chin *et al*[1] focuses on the detection of metastatic spread of non-small cell lung cancer to the mediastinal lymph nodes. They assessed two non-invasive imaging modalities – computed tomography (CT) and positron emission tomography (PET) with radiolabelled fluoro-2-deoxyglucose (^{18}FDG) – using histopathology of the nodes following surgical exploration of the mediastinum as the "gold standard". Radiographic computed tomography, as we know, gives excellent anatomical resolution (down to 1·0 mm or so with appropriate algorithms) but no cellular specificity apart from fat, water, and bone differentiation on the basis of Hounsfield numbers. For the assessment of malignancy in lymph nodes, CT relies solely on size. In a meta-analysis of 32 studies[2] where a diameter of 5–10 mm was chosen as the threshold the accuracy of CT scanning was 0·75, increasing to 0·86 at >10 mm. However, many larger nodes (20–40 mm) may be negative if there has been chronic intrapulmonary infection. Magnetic resonance imaging is no better than CT scanning in this context.

Imaging methods which are more cell or tissue specific are needed – for example, monoclonal antibodies which recognise tumour-specific cell surface antigens, or markers of an increased mitotic index (DNA probes such as ^{11}C-thymidine) or of protein turnover (^{11}C-methionine). Fortunately, a simpler solution is to hand. Cancer cells, along with phagocytes, have a very high glucose uptake for reasons which will be discussed later. 2-deoxyglucose (2-DOG) is an analogue of glucose whose intracellular metabolism is blocked when conversion to 2-DOG-6-phosphate occurs. If 2-DOG is radiolabelled with fluorine-18 (a positron emitting isotope with a physical half life of 110 minutes), the accumulation of radioactivity in any tissue reflects its ^{18}FDG-6-phosphate content and its metabolic rate for glucose.

Cellular uptake of 2-fluoro-[18]-deoxyglucose (^{18}FDG)[3]

2-deoxy-D-glucose differs from glucose only in the replacement of one hydroxyl group by a hydrogen atom.

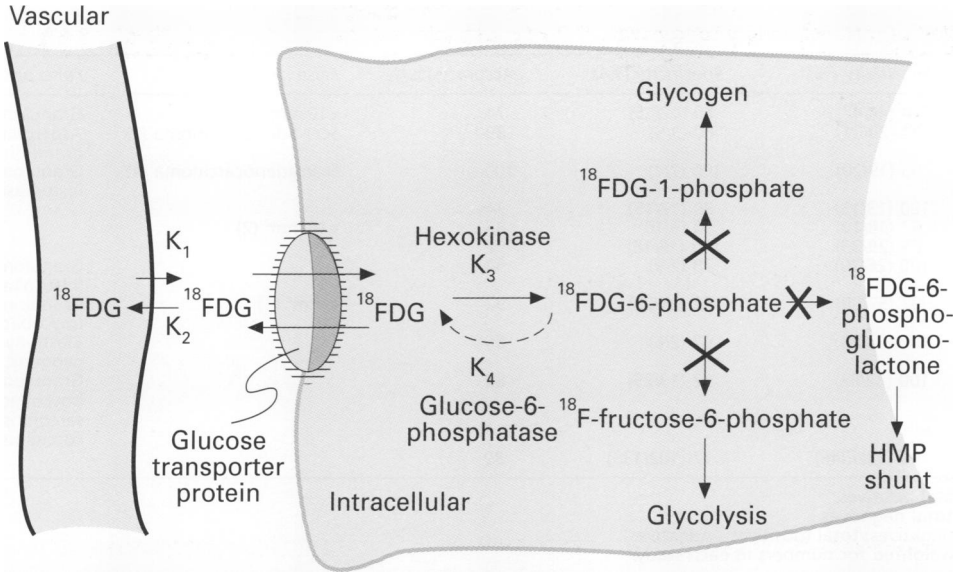

Figure 1 Schematic diagram of cellular uptake of vascular ^{18}FDG and its conversion to ^{18}FDG-6-phosphate; further metabolism does not take place.

The body treats 2-DOG in the same way until a point in the glycolytic pathway where its different structure prevents further metabolism (fig 1). 2-DOG and glucose compete for the same membrane-bound transporter protein and the same enzyme (hexokinase) for phosphorylation (to 2-DOG-6-phosphate). Glucose then follows several enzymatically driven pathways: (1) via phosphoglucomutase to glycogen, (2) via G-6-phosphate dehydrogenase (G6PD) into the hexose monophosphate shunt, and (3) via phosphohexoisomerase down the glycolytic path to pyruvate. None of these enzymes can catalyse the structurally slightly different DOG-6-phosphate. The only metabolic avenue left for DOG-6-phosphate is the back reaction (k_4) catalysed by G-6-phosphatase. Heart, brain, and neoplastic tissue contain very little phosphatase and their radioactive signal 60 minutes after an ^{18}FDG injection is entirely "metabolic" – that is ^{18}FDG-6-phosphate. Liver, kidney, intestine, and muscle have higher G-6-phosphatase levels and accumulate less ^{18}FDG-6-phosphate than their metabolism would warrant. These organs contribute only a low level of background radioactivity which helps to highlight the FDG-PET signal from cancer and inflammation.

Figure 2A shows the plasma and tissue kinetics of ^{18}FDG following intravenous injection. The Patlak plot (fig 2B) of the tissue:plasma ^{18}FDG ratio against the integrated plasma:instantaneous ^{18}FDG concentration (a "normalised" input function) gives a straight line whose slope represents metabolic rate; the intercept is the extracellular distribution volume of free ^{18}FDG.

Why do cancers have a high glucose uptake?

The glucose metabolic uptake is increased in all types of cancer including breast, colon, lung, melanoma, astrocytoma, sarcoma, lymphoma (reviewed by Rege *et al*[4]). The increase in metabolism appears generally indifferent to histological type or pattern, at least in the lung.[5] The only normal tissues whose ^{18}FDG uptake approaches that of neoplastic tissue are the brain, myocardium (in the non-fasted state), and inflammatory tissue.

Cancer cells have a very different method of energy production from normal mammalian cells. The ratio of aerobic to anaerobic production of adenosine triphosphate (ATP) in the adult kidney and liver is about 100, compared with 1·0 in neoplastic cells.[6] Otto Warburg,[6] the pioneer of this subject, conceived neoplastic transformation as a loss of mitochondrial enzymes and

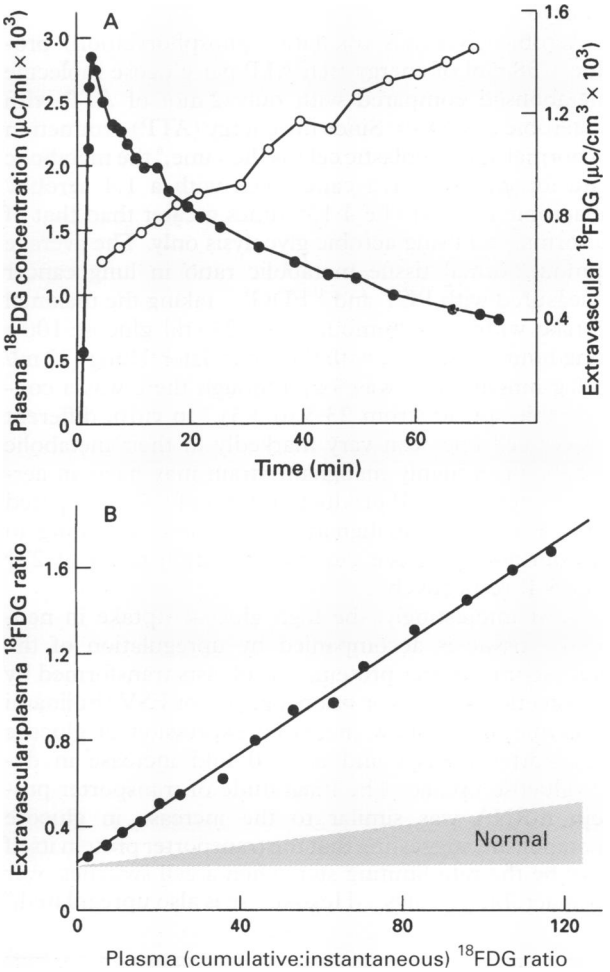

Figure 2 (A) Plasma (●) and extravascular lung (○) ^{18}FDG concentrations plotted against time following intravenous injection at time zero. (B) Transformation of above data where abscissa represents area under the plasma curve (cumulative) up to time t divided by plasma level at time t. Slope is proportional to metabolic rate for glucose. Normal range is shaded. Reproduced from Brudin et al[12] *with permission.*

Table 1 Detection of intrapulmonary cancer with ^{18}FDG-PET scanning

Reference no.	Sensitivity (%)*	Specificity (%)†	Accuracy (%)‡	False negatives	False positives
16	94 (44/47)	80 (12/15)	74	<10 mm² (2)	Granulomas (3)
17	94 (29/31)	60 (3/5)	89	Scar adenocarcinoma (1)	Aspergillosis (1), granuloma (1)
18	95 (19/20)	100 (7/7)	100	Scar adenocarcinoma (1)	Granulomas (2), histoplasmosis (1)
19	100 (13/13)	80 (12/15)	74		
20	83 (10/12)	90 (9/10)	86	<10 mm² (2)	
21	89 (29/33)	100 (18/18)	92		
22	100 (26/26)	78 (7/9)	94		Granulomas (2) (histoplasmosis)
23	97 (57/59)	82 (23/28)	92	4 mm² (1)	Granuloma (1) (mycobacteria)
24	100 (23/23)	67 (2/6)	86		Blastomycosis (1), pyogenic abscess (1)
25	100 (82/82)	52 (13/25)	89		Granuloma (7) [mycobacteria (3), sarcoidosis (4)], coccidiomycosis (3)
Mean	96 (332/346)	77 (102/133)	89		

*^{18}FDG positives/total positives.
†^{18}FDG negatives/total negatives.
‡FDG (positives + negatives)/total (positives + negatives).
Mean values are weighted for numbers in each study.

a reversion to a dedifferentiated cell employing the alternative, but more primitive, means of energy production – that is, anaerobic glycolysis or "fermentation". We associate lactate production with yeast cells but it is also a feature of the early stage of development of the embryo.

Aerobic glycolysis (oxidative phosphorylation) produces 38 mol of energy-rich ATP per glucose molecule metabolised compared with only 2 mol of ATP with anaerobic glycolysis. Since the energy (ATP) production of normal and neoplastic cells is the same,[6] the metabolic rate for glucose for a cancer cell with a 1:4 aerobic/anaerobic ratio will be 4·13* times greater than that of a normal cell using aerobic glycolysis only. The average tumour/normal tissue metabolic ratio in lung cancer (measured with PET and ^{18}FDG) – taking the maximal uptake within the tumour area (293 ml glucose/100 g lung/hour) compared with the contralateral lung (32 ml/100 g lung/hour) – was 9·2, although there was a considerable spread (from 23·3 to 3·5).[5] In vitro, different cancer cell lines can vary markedly in their metabolic behaviour; a highly malignant strain may have an aerobic/anaerobic ATP production ratio of 0·71 compared with 3·5 for low malignancy cells[6] (corresponding to tumour:normal tissue glucose utilisation ratios of 27† and 5·4, respectively).

Most interestingly, the high glucose uptake in neoplastic tissue is accompanied by upregulation of the glucose transporter protein. Fibroblasts transformed by transfection with *ras* or *src* oncogenes[7] or FSV (Fujinami sarcoma virus)[8] show increased expression of glucose transporter mRNA and a 4–10 fold increase in deoxyglucose uptake. The magnitude of transporter protein mRNA was similar to the increase in glucose metabolism, suggesting that the transporter protein itself may be the rate limiting step when a cell switches over to anaerobic glycolysis. Hexokinase is also upregulated.[9]

* Per 5 mol glucose, a 1:4 aerobic/anaerobic metabolic ratio produces 38 + (2 × 4) = 46 mol ATP which, by aerobic glycolysis, requires 46/38 = 1·2 mol glucose. 1:4 aerobic/anaerobic ratio consumes 4·13 (5/1·21) more glucose than aerobic metabolism per se.

† Given an aerobic/anaerobic ratio of 0·71 for ATP production, 0·71 mol ATP require 0·0187 mol glucose (aerobic) and 1·0 mol ATP requires 0·5 mol glucose (anaerobic). The anaerobic/aerobic glucose consumption ratio = 26·7 (0·5/0·0187).

PHAGOCYTES

Neutrophils, eosinophils, and macrophages are also deficient in oxidative respiratory enzymes and have a high glucose uptake per mol ATP produced. In an experimental model of acute lobar pneumonia in rabbits (instillation of *Streptococcus pneumoniae* in the right upper lobe), the peak uptake of ^{18}FDG at 15 hours was 6–19 times greater than the unaffected left upper lobe.[10] In humans, ^{18}FDG uptake is high in acute pneumonia but not in the chronic bacterial sepsis of bronchiectasis.[11] High uptakes are also seen in sarcoidosis[12] and, to a lesser extent, in cryptogenic fibrosing alveolitis.[13] Chronic granulomatous inflammation is the commonest cause for false positive ^{18}FDG signals in imaging of lung cancer and metastatic mediastinal nodes.

Cellular origin of the ^{18}FDG signal in lung cancer

Cancers (and metastatic lymph nodes) may be very heterogeneous with areas of necrosis, normal tissue, and inflammatory infiltrates (containing macrophages, neutrophils, and fibroblasts) coexisting with neoplastic cells. Kubota *et al*[14] have studied, with macro- and micro-autoradiography, the uptake of ^{18}FDG in mouse tumours induced by implantation of FM3A mammary carcinoma cells. The grain count (per 100 mm²) was up to 3·5 times more intense in those parts of the tumour where macrophages were infiltrating an area of tumour necrosis. Nevertheless, the bulk of the ^{18}FDG signal (71%) originated from neoplastic tissue because these cells were the most numerous. Brown *et al*[15] in a similar autoradiographic study of ovarian cancer xenografts in nude mice, found selective accumulation of ^{14}C-DOG in viable cancer cells but none in neutrophils within the tumours. Neither study found any ^{18}FDG uptake in necrotic areas which is in agreement with low ^{18}FDG activity in the central regions of some tumours in FDG-PET scans.[5]

^{18}FDG-PET scans and intrapulmonary malignancies

Table 1 sets out the results of 10 studies which have looked at the efficiency of ^{18}FDG-PET scans in the

Table 2 Efficiency of ^{18}FDG-PET scanning compared with CT scanning for the detection of malignancy in mediastinal lymph nodes (verified by surgical excision) in cases of proven lung cancer

Reference no.	^{18}FDG scanning			Radiographic CT scanning		
	Sensitivity (%)*	Specificity (%)†	Accuracy (%)‡	Sensitivity (%)*	Specificity (%)†	Accuracy (%)‡
28	82 (9/11)	81 (13/16)	81	64 (7/11)	44 (7/16)	52
25	100 (16/16)	100 (16/16)	100	81 (13/16)	56 (9/16)	69
1	78 (7/9)	81 (17/21)	80	56 (5/9)	86 (18/21)	77
29	92 (11/12)	100 (10/10)	95	58 (7/12)	80 (8/10)	68
Mean	96 (43/48)	89 (56/63)	88	67 (32/48)	67 (42/63)	66
29§	73 (8/11)	76 (22/29)	75	27 (3/11)	86 (25/29)	70

*^{18}FDG positives/total positives.
†^{18}FDG negatives/total negatives.
‡^{18}FDG (positives + negatives)/total (positives + negatives)
§Hilar nodes only.
Mean values are weighted for numbers in each study.

detection of lung cancers. In all, only 14 out of 346 cancers were missed, and these were mostly <1 cm in size. False negatives have also occurred in unusual cancers such as scar adenocarcinomas (table 1), carcinoid tumours (two),[1] and in a pulmonary infarct with a small rim of cystadenocarcinoma.[1] There were 31 false positives out of 133 cases (23%); at least two thirds of these turned out to be granulomatous disease which, in a North American context, included mycoses which are rare in Europe (table 1). The greater benefit, perhaps, from ^{18}FDG-PET scans in imaging intrapulmonary lesions is their high negative predictive value.

QUANTITATION

The ^{18}FDG-PET scans have been normalised in terms of a standardised uptake ratio or value (SUR or SUV), also called a differential uptake ratio (DUR), which is:

region of interest radioactivity (mBq/ml)/injected dose (mBq)/body weight (kg)

In five studies[18 19 21 23 24] involving 141 positive PET scans (all cancer confirmed) the SUR varied from 5·55 to 6·89 (mean 6·2) with a large coefficient of variation (CV) of 45–54%. In benign lesions the SUR averaged 1·6 (range 0·56–2·72). In none of these studies was there a clear separation between the benign and malignant groups for SUR because benign lesions are frequently "inflammatory" in nature. Hubner *et al*[24] looked at the spread of SURs in non-malignant tissues and found the highest values in the unfasted myocardium (7·5 (2·4–16·2)) and in active inflammation (6·1 (2·6–10·7)). Cerebral tissue values, which are also high, were not reported. Not surprisingly, the brain and myocardium are prominent on ^{18}FDG-PET scans. Fasting for 4–6 hours reduces the myocardial signal. Normal lung had one of the lowest values (0·74 (0·1–1·9)) which makes the detection of neoplastic "hot spots" easier.

The SUR is a relatively crude index because the tissue uptake has not reached a steady state 60 minutes after injection (fig 2A) when counting takes place. The Patlak plot (fig 2B) discriminates between uninvolved and involved (that is, malignant) lesions better than the SUR[24] – Patlak plot: 8·2 (3·8) ml/min/100 g for involved, 2·1 (1·7) for uninvolved; SUR: 6·9 (3·8) for involved, 2·7 (1·6) for uninvolved lung.[24] Using a cut-off (benign versus malignant) for SUR of 3·5, and for the Patlak plot of 4·0, the sensitivity, specificity, and accuracy for SUR was 82% (18/22), 81% (50/62), and 81%, respectively compared with 91% (20/22), 90% (56/62), and 91%, respectively, for the Patlak plot.[24] Thus, in comparison with table 1 (where PET diagnoses were qualitative), quantitation with the Patlak plot may increase the specificity of ^{18}FDG-PET scans, reducing the number of false positives by 15%, but the extra effort of repeated scanning and continuous monitoring of vascular ^{18}FDG levels is unlikely to find favour with most clinical PET units.

PLASMA GLUCOSE

The uptake of ^{18}FDG is influenced by plasma glucose levels. The behaviour of tissues to a glucose load depends on their insulin sensitivity (high for muscle, low for brain) and whether their glucose transporter protein is saturated at resting glucose levels. Langen *et al*[26] repeated ^{18}FDG-PET scans in 15 patients with bronchial carcinomas after raising plasma glucose from 85 to 168 mg/100 ml (4·7 to 9·3 mmol/l) with an intravenous infusion of 20% glucose. There was a 42% fall in SUR values during the glucose infusion, although the slope of the Patlak plot did not change. Lindholm *et al*,[27] in a study of five patients with head and neck cancer, found a similar reduction (40%) with oral glucose loading with a 25% decrease in glucose metabolic rate. After the glucose load, plasma insulin levels increased sixfold. In the normal neck muscles SUV doubled and the glucose metabolic rate increased sixfold. This was in marked contrast to the behaviour of the cancers which, like some other tissues such as brain, intestinal mucosa, and kidney tubules, did not increase their glucose transport when insulin levels rose. The slope of the Patlak plot should fall. Overall, normalising the SUR to the plasma glucose level eliminated the hyperglycaemic effect, though significant differences remained in some patients. It is usual to scan with ^{18}FDG-PET in the fasting state, but there is no need to "clamp" the plasma glucose at a particular level. Plasma glucose should be checked in diabetic patients.

Detection of mediastinal metastases

With regard to intrathoracic staging, clinicians are interested in the positive as well as the negative predictive value of ^{18}FDG-PET scans. The results from four studies[1 25 28 29] are presented in table 2 in which ^{18}FDG-PET scans are compared with CT scans using histopathology of nodes removed at thoracotomy as the "gold standard". The false negative (sensitivity) and false positive (specificity) rate is consistently lower for ^{18}FDG-PET than for CT scanning. This is not surprising since the CT scan relies on size only, whereas ^{18}FDG-PET measures a functional change.

In the introductory article by Chin *et al*[1] the malignant lymph nodes were assigned to a particular nodal station (for ^{18}FDG-PET and CT scans and at surgery) according to the ATS map.[30] Although agreement between ^{18}FDG-PET and CT nodal location and the surgically labelled station was poor, the nodal loci in each circumstance were generally within one level. Two groups have published co-registration images in which the ^{18}FDG-PET and CT scans appear colour coded as overlays – an anatometabolic fusion image!

Patz *et al*[29] compared the specificity of ^{18}FDG-PET scans for mediastinal versus hilar nodes (table 2). All ^{18}FDG-PET positive mediastinal nodes were malignant, but seven out of 29 ^{19}FDG-PET positive hilar nodes were "reactive" with significant inflammatory change (sinus histiocytosis).

^{18}FDG-PET and extrapulmonary metastases

Unsuspected lesions in the contralateral lung shown by ^{18}FDG-PET scanning have led to cancellation of surgical exploration.[1] Lewis *et al*[31] found extrathoracic ^{18}FDG uptake in 11 of 34 patients with non-small cell lung cancer (all had a positive local ^{18}FDG signal) including extrathoracic lymph nodes (5), brain (3), bone (2), and skin (1). These findings influenced subsequent management. Rege *et al*[4] detected extrathoracic spread in three cases of lung cancer (brain (2), liver (1), pelvis (2)), and cervical and inguinal nodal involvement in a patient with positive hilar nodes due to Hodgkin's disease.

^{18}FDG-6-phosphate is excreted in the urine. Whole body scanning shows regions of high activity in the bladder and renal calyces (especially with intrarenal hold-up). For a thorough examination of the pelvis, if indicated, urine must be voided or the bladder catheterised just before the pelvis is scanned.

Detection of recurrent tumour

^{18}FDG-PET scanning has high sensitivity and specificity in the detection of recurrent cancer. In five studies[23 24 32–34] (219 patients) recurrent cancer was missed in only four of 139 cases (3%). The false positive rate was 15 of 80 cases (81% specificity) giving an overall accuracy of 91%. The mean SUV in three studies[23 32 34] was 8·1 for cancer recurrence and 2·4 for no tumour. False positives occurred with radiation pneumonitis (1), macrophage accumulation around necrotic tissue (1), reactive mesothelial cells (2), and acute inflammation (2). Frank *et al*[33] found the sensitivity and specificity of ^{18}FDG-PET to be 100% and 89%, respectively, compared with 67% and 85% for CT scanning, giving overall accuracies of 93% and 82%, respectively.

Technical aspects

The first study of lung cancer with ^{18}FDG-PET[5] used an ECAT II (CTI, Knoxville) with a single ring of scintillation detectors. It was not a diagnostic machine. Considerable advances have occurred since 1985 in PET scanner design and sensitivity. The ECAT V (CTI 931–08)[4 22] had eight rings of bismuth germinate

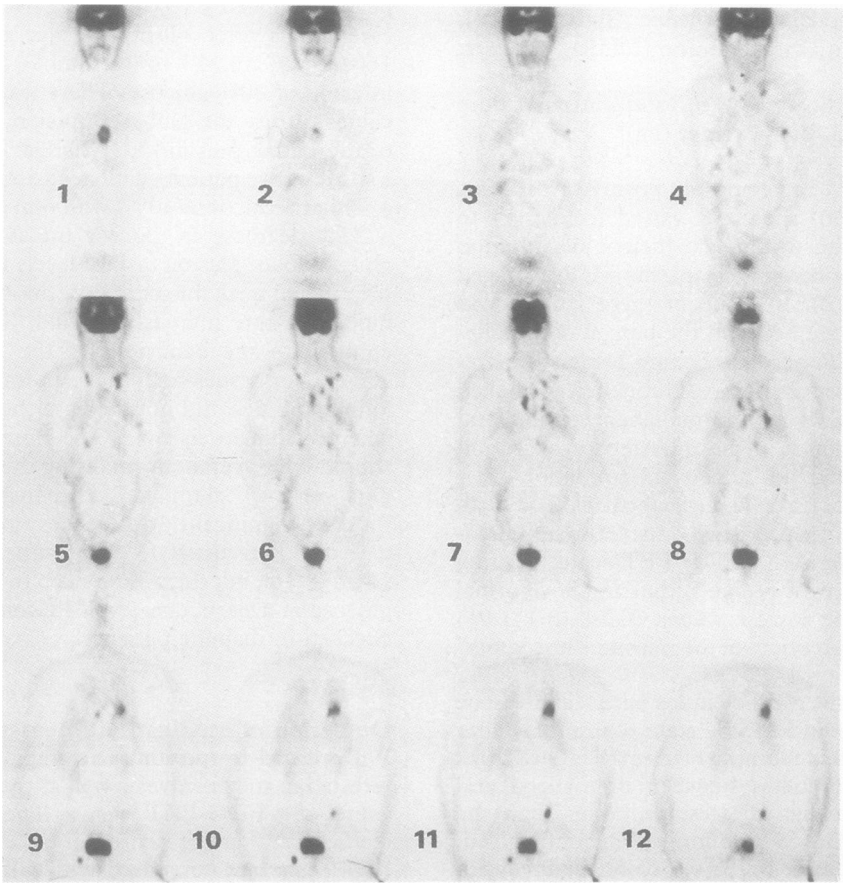

Figure 3 Coronal images of ^{18}FDG uptake using the ECAT-ART rotating PET scanner from ventral (top left, image 1) to dorsal (bottom right, image 12) of a patient with disseminated squamous cell carcinoma of the bronchus. The primary lesion is seen in the left lower lobe (bottom row, images 9–12). ^{18}FDG uptake in the mediastinal and supraclavicular nodes bilaterally is seen in the middle row (images 5–8); uptake in both adrenal glands is visible (images 5 and 6). Focal uptake in the left iliac crest (images 10–12) and right ischium (images 8–11), lower sternum (images 1 and 2), left fifth rib (image 4) and anterior part of the right eighth rib (images 3 and 4) corresponded to abnormalities seen on a ^{99m}Tc-pyrophosphate bone scan. (From Nuclear Medicine Division, Department of Radiology, Hammersmith Hospital).

LEARNING POINTS

* ^{18}F-deoxyglucose (^{18}FDG) is taken up with great avidity by neoplastic cells and phagocytes because they are primitive "fermenting" cells with a high anaerobic/aerobic metabolic ratio.
* FDG-PET scans are highly sensitive in the detection of lung cancer with 14 missed diagnoses out of 346 cases.
* FDG-PET scans are very specific in lung cancer detection with only a 23% false positive rate, mostly due to granulomatous disease.
* In the detection of malignancy in mediastinal (but not hilar) lymph nodes, FDG-PET scanning has an overall accuracy of 88% compared with 66% for CT scanning. In 48 cases there were five "missed" diagnoses with FDG-PET scanning compared with 16 with CT scans.
* FDG-PET scanning is likely to have a major impact in clinical oncology. It could assist the chest physician in the management of pulmonary nodules.

(BGO) detectors made up in blocks sliced into eight sections from which 15 planes of information, 6·75 mm thick, could be derived using "cross-plane" information between adjacent rings. This covers a distance of 10 cm, about 50% of the supine lung at mid tidal volume. Better resolution comes from the 16 slice machine[1 25] which gives 31 planes, 3·75 mm thick, and an axial field of view of 10·5 cm. The within plane spatial resolution is generally quoted as 5·5–6·5 mm which is appropriate for the mediastinum. In the lung the spatial resolution will be about 15 mm because of breathing motion and because of the reduced "stopping power" of lung tissue for positron emission. Siemens/CTI have introduced the EXACT L17 PET scanner with 47 planes (24 detector rings), 3·5 mm thick, with an axial field of view of 16·2 cm.[24] Others [23 29] have used the GE 4096 Plus or Advance; the former has 15 planes and the latter stretches to 35 planes (18 detector rings) with a 15 cm field of view.

With an axial distance of 16·2 cm up to eight contiguous scans (because of overlap) would be needed to cover 50% (neck to pelvic floor) of a body 170 cm in height. Scanning time would be about 60 minutes. Transmission scans with a ^{68}Ge/^{68}Ga ring surrounding the subject give an attenuation correction for the different tissue densities within transaxial body slices. This enhances the resolution and definition of the ^{18}FDG image. Most centres use a transmission scan for thoracic imaging which is essential for the SUV calculation. It adds about 20 minutes to the study so the total scanning time might extend to 80 minutes.

The Siemens/CTI ECAT-ART rotating PET camera is a very interesting development. The blocks of BGO detectors ($54 \times 54 \times 20$ mm) are sectioned into an 8×8 array (similar to the EXACT scanner), each detector crystal measuring $6{\cdot}4 \times 6{\cdot}4 \times 20$ mm. There are only three blocks in the axial direction from which 24 (3×8) rings and 47 reconstructed planes are obtained. Circular rings of detectors are extremely expensive. In ECAT-ART two opposed banks of detectors, covering an arc of 160°, rotate once every two seconds. Thus, the number of detector elements is reduced by 160/360 (44%). This reduces the cost by up to 50%. Data acquisition is in 3D mode rather than the conventional 2D mode. This compensates for the loss of detector number and gives equivalent performance characteristics. Figure 3 shows a series of images from the ECAT-ART scanner.

Future prospects

FDG-PET will have a big impact in cancer staging and in monitoring the response to therapy. A single body scan with FDG-PET might replace some of the bone, CT, and MRI scans and the ultrasound imaging currently used in the examination of a patient with suspected or proven cancer. The FDG-PET scan could be very useful to the chest physician in the investigation of peripheral pulmonary nodules. The high negative predictive value of FDG-PET scanning means that a "cold" lesion is very unlikely to be malignant and can safely be watched without recourse to fine needle aspiration.

Phagocytes share the same avidity for glucose as neoplastic cells. Like the radioactive gallium scan which preceded it, the FDG-PET scan will give a positive signal in inflammatory disease (especially when activated macrophages accumulate in granulomas) as well as in cancers. If the clinical context is appropriately chosen, confusion does not often occur; witness the high sensitivity and specificity of FDG-PET scanning in lung cancer detection (tables 1 and 2). The role of FDG-PET in the diagnosis and monitoring of mycobacterial and sarcoid disease remains to be assessed.

The negative aspects of clinical FDG-PET scanning are its cost (similar to an MRI scanner) and the need for access to a cyclotron for the production of ^{18}F-deoxyglucose. Since ^{18}F has a physical half life of nearly two hours (110 minutes), and since only 190–370 MBq needs to be injected for an FDG scan, a cyclotron which can make 7400 MBq of ^{18}FDG (quite feasible these days) has a time period of six hours (three half lives) for delivery of 925 MBq to the PET scanner. Thus, the medical cyclotrons in the UK could provide a countrywide service.

I am grateful to Dr Helen Young and Professor AM Peters for loan of the images from the ECAT-ART PET scanner in the Nuclear Medicine Division of the Department of Radiology at Hammersmith Hospital.

1 Chin R, Ward R, Keyes JW, Choplin RH, Reed JC, Wallenhaupt S, *et al.* Mediastinal staging of non-small-cell lung cancer with positron emission tomography. *Am J Respir Crit Care Med* 1995;**152**:2090–6.
2 Dales RE, Stark RM, Raman S. Computed tomography to stage lung cancer: approaching a controversy using meta-analysis. *Am Rev Respir Dis* 1990;**141**:1096–101.
3 Sokoloff L, Reivich M, Kennedy C, *et al.* The ^{14}C deoxyglucose methods for the measurement of local cerebral glucose utilization in man. *J Neurochem* 1977;**28**:897–916.
4 Rege SD, Hoh CK, Glaspy JA, *et al.* Imaging of pulmonary mass lesions with whole-body positron emission tomography and fluorodeoxyglucose. *Cancer* 1993;**72**:82–90.
5 Nolop KB, Rhodes CG, Brudin LH, *et al.* Glucose utilization in vivo by human pulmonary neoplasms. *Cancer* 1987;**60**:2682–9.
6 Warburg O. On the origin of cancer cells. *Science* 1956;**123**:309–14.
7 Flier JS, Mueckler MM, Usher P, Lodish HF. Elevated levels of glucose transport and transporter messenger RNA are induced by *ras* or *src* oncogenes. *Science* 1987;**235**:1492–5.
8 Birnbaum MJ, Haspel HC, Rosen OM. Transformation of rat fibroblasts by FSV rapidly increases glucose transporter gene transcription. *Science* 1987;**235**:1495.
9 Monakhov NK, Neistadt EL, Shavlovskil MM. Physicochemical properties and isoenzyme composition of hexokinase from normal and malignant human tissues. *J Natl Cancer Inst* 1978;**67**:27–34.
10 Jones HA, Clark RJ, Rhodes CG, Schofield JB, Krausz T, Haslett C. In vivo measurement of neutrophil activity in experimental lung inflammation. *Am J Respir Crit Care Med* 1994;**149**:1635–9.
11 Jones HA, Sriskandan S, Peters AM, Krausz T, Pride NB, Haslett C. Metabolic activity of neutrophils is distinct from migration in lobar pneumonia and bronchiectasis. *Am J Respir Crit Care Med* 1995;**151**: A343.
12 Brudin LH, Valind SO, Rhodes CG, *et al.* Regional glucose uptake in patients with sarcoidosis. *Eur J Nucl Med* 1994;**21**:297–305.
13 Pantin CF, Valind SO, Sweatman M, *et al.* Measures of the inflammatory response in cryptogenic fibrosing alveolitis. *Am Rev Respir Dis* 1988; **138**:1234–41.
14 Kubota R, Yamada S, Kubota K. Intratumoral distribution of fluorine-18-fluorodeoxyglucose in vivo: high accumulation in macrophages

and granulation tissues studied by microautoradiography. *J Nucl Med* 1992;**33**:1972–80.
15. Brown SR, Fisher SJ, Wahl RL. Autoradiographic evaluation of the intra-tumoral distribution of 2-deoxy-D-glucose and monoclonal antibodies in xenografts of human ovarian adenocarcinoma. *J Nucl Med* 1993;**34**:75–82.
16 Scott WJ, Schwabe JL, Gupta NC, Dewan NA, Reeb SD, Sugimoto JT. Positron emission tomography of lung tumours and mediastinal lymph nodes using [18F]fluorodeoxyglucose. *Ann Thorac Surg* 1994; **58**:698–703.
17 Slosman DO, Spiliopoulos A, Couson F, *et al*. Satellite PET and lung cancer: a prospective study in surgical patients. *Nucl Med Commun* 1993;**14**:955–61.
18 Dewan NA, Gupta NC, Redepenning LS, Phalen JJ, Frick MP. Diagnostic efficacy of PET-FDG imaging in solitary pulmonary nodules. Potential role in evaluation and management. *Chest* 1993;**104**:997–1002.
19 Gupta NC, Frank AR, Dewan NA, *et al*. Solitary pulmonary nodules: detection of malignancy with PET with 2-[F-18]-fluoro-2-deoxy-D-glucose. *Radiology* 1992;**184**:441–4.
20 Kubota K, Matsuzawa T, Fujiwara T, *et al*. Differential diagnosis of lung tumor with positron emission tomography: a prospective study. *J Nucl Med* 1990;**31**:1927–32.
21 Patz EF, Lowe VJ, Hoffman JM, *et al*. Focal pulmonary abnormalities: evaluation with F-18 fluorodeoxyglucose PET scanning. *Radiology* 1993;**188**:487–90.
22 Dewan NA, Reeb SD, Gupta NC, Gobar LS, Scott WJ. PET-FDG imaging and transthoracic needle lung aspiration biopsy in evaluation of pulmonary lesions. A comparative risk-benefit analysis. *Chest* 1995; **108**:441–6.
23 Duhaylongsod FG, Lowe VJ, Patz EF, Vaughn AL, Coleman RE, Wolfe WG. Detection of primary and recurrent lung cancer by means of F-18 fluorodeoxyglucose positron emission tomography. *J Thorac Cardiovasc Surg* 1995;**110**:130–9.
24 Hubner KF, Buonocore E, Singh SK, Gould HR, Cotten DW. Characterization of chest masses by FDG positron emission tomography. *Clin Nucl Med* 1995;**20**:293–8.
25 Sazon DAD, Siverio SM, Soo Hoo GW, *et al*. Fluorodeoxyglucose-positron emission tomography in the detection and staging of lung cancer. *Am J Respir Crit Care Med* 1996;**153**:417–21.
26 Langen KJ, Braun U, Rota-Kops E, *et al*. The influence of plasma glucose levels on fluorine-18-fluorodeoxyglucase uptake in bronchial carcinomas. *J Nucl Med* 1993;**34**:355–9.
27 Lindholm P, Minn H, Leskinen-Kallio S, Bergman J, Ruotsalanen U, Joensuu H. Influence of blood glucose concentration on FDG uptake in cancer – a PET study. *J Nucl Med* 1993;**34**:1–6.
28 Wahl RL, Quint LE, Greenough RL, Meyer CR, White RI, Orringer MB. Staging of mediastinal non-small cell lung cancer with FDG PET, CT, and fusion images: preliminary prospective evaluation. *Radiology* 1994;**191**:371–7.
29 Patz EF, Lowe VJ, Goodman PC, Herdon J. Thoracic nodal staging with PET imaging with ^{18}FDG in patients with bronchogenic carcinoma. *Chest* 1995;**108**:1617–21.
30 American Thoracic Society. Clinical staging of primary lung cancer. *Am Rev Respir Dis* 1983;**127**:659–64.
31 Lewis P, Griffin S, Marsden P, *et al*. Whole-body 18-F-fluorodeoxyglucose positron emission tomography in preoperative evaluation of lung cancer. *Lancet* 1994;**344**:1265–6.
32 Patz EF, Lowe VJ, Hoffman JM, Paine SS, Harris LK, Goodman PC. Persistent or recurrent bronchogenic carcinoma: detection with PET and 2-[F-18]-fluoro-2-deoxy-D-glucose. *Radiology* 1994;**191**:379–82.
33 Frank A, Lefkowitz D, Jaeger S, *et al*. Decision logic for retreatment of asymptomatic lung cancer recurrence based on positron emission tomography findings. *Int J Radiat Oncol Biol Phys* 1995;**32**:1495–512.
34 Inoue T, Kim EE, Komaki R, *et al*. Detecting recurrent or residual lung cancer with FDG-PET. *J Nucl Med* 1995;**36**:788–93.

THORAX

18F-fluorodeoxyglucose PET scans in lung cancer.

J M Hughes

*Thorax*1996 51: S16-S22
doi: 10.1136/thx.51.Suppl_2.S16

Notes